Injectable Carbon Nanotube-Functionalized Reverse Thermal Gel Promotes Cardiomyocytes Survival and Maturation

Brisa Peña[†,iD], **Susanna Bosi**[‡], **Brian A. Aguado**[∥], **Daniele Borin**[§], **Nikki L. Farnsworth**[⊥], **Evgenia Dobrinskikh**[#], **Teisha J. Rowland**[†], **Valentina Martinelli**[∇], **Mark Jeong**[†], **Matthew R. G. Taylor**[†], **Carlin S. Long**[†], **Robin Shandas**[⊥], **Orfeo Sbaizero**[§], **Maurizio Prato**[‡,○,◆], **Kristi S. Anseth**[∥], **Daewon Park**[⊥,*], and **Luisa Mestroni**[†,*]

[†]Cardiovascular Institute, University of Colorado Denver Anschutz Medical Campus, School of Medicine, Division of Cardiology, 12700 E. 19th Avenue, Bldg. P15, Aurora, Colorado 80045, United States

[‡]Department of Chemical and Pharmaceutical Sciences, University of Trieste, Trieste 34127, Italy

[§]Department of Engineering and Architecture, University of Trieste, Trieste 34127, Italy

[∥]Department of Chemical and Biological Engineering and Howard Hughes Medical Institute and the BioFrontiers Institute, University of Colorado at Boulder, 3415 Colorado Avenue, Boulder, Colorado 80309, United States

[⊥]Bioengineering Department, University of Colorado Denver Anschutz Medical Campus, Bioscience 2 1270 E. Montview Avenue, Suite 100, Aurora, Colorado 80045, United States

[*]**Corresponding Authors**, Phone: 303-724-6947. daewon.park@ucdenver.edu. (D.P.) Phone: 303-724-0858. luisa.mestroni@ucdenver.edu. (L.M.).

ORCID

Brisa Peña: 0000-0003-4224-6626

ASSOCIATED CONTENT

Supporting Information

The Supporting Information is available free of charge on the ACS Publications website at DOI: 10.1021/acsami.7b11438.

Different MWCNT-COOH dispersed in DMF. Commercial MWCNT-COOH and our home-synthesized MWCNT-COOH (PDF)

Sol to gel phase transition injection at 37 °C of the RTG-lysine system using a 31 gauge needle. Injection is made in water, and polymer was dissolved in water at 1.5% (w/w) (AVI)

Sol to gel phase transition injection at 37 °C of the RTGCNT system using a 31 gauge needle. Injection is made in water, and polymer was dissolved in water at 1.5% (w/w) (AVI)

Spontaneous intracellular calcium oscillations of NRVM cultured for 21 d in the 3D RTG-CNT scaffold (AVI)

Spontaneous intracellular calcium oscillations of NRVM cultured for 21 d in the 3D RTG-lysine scaffold (AVI)

Spontaneous intracellular calcium oscillations of NRVM cultured for 21 d in 2D gelatin control (AVI)

Author Contributions

The manuscript was written through contributions of all authors. All authors have given approval to the final version of the manuscript. B.P. performed all the polymer synthesis experiments, SEM characterization, cell isolation, in vitro cell studies, cell staining, calcium transients, and cell imaging. S.B. performed the CNT synthesis and characterization. B.A. characterized the mechanical properties of the hydrogels. D.B. performed the AFM analysis. N.L.F. helped to analyze the resistance properties of the materials. E.D. provided her valuable advice in the calcium transients experiments and analysis.

The authors declare no competing financial interest.

#Department of Medicine, University of Colorado Denver Anschutz Medical Campus, 12700 E. 19th Avenue, Bldg. P15, Aurora, Colorado 80045, United States

∇International Center for Genetic Engineering and Biotechnology, Area Science Park, Padriciano 99, Trieste 34149, Italy

○Carbon Nanobiotechnology Laboratory, CIC biomaGUNE, Paseo de Miramón 182 20009, Donostia-San Sebastián 20009, Spain

◆Basque Foundation for Science, Ikerbasque, Bilbao 48013, Spain

Abstract

The ability of the adult heart to regenerate cardiomyocytes (CMs) lost after injury is limited, generating interest in developing efficient cell-based transplantation therapies. Rigid carbon nanotubes (CNTs) scaffolds have been used to improve CMs viability, proliferation, and maturation, but they require undesirable invasive surgeries for implantation. To overcome this limitation, we developed an injectable reverse thermal gel (RTG) functionalized with CNTs (RTG-CNT) that transitions from a solution at room temperature to a three-dimensional (3D) gel-based matrix shortly after reaching body temperature. Here we show experimental evidence that this 3D RTG-CNT system supports long-term CMs survival, promotes CMs alignment and proliferation, and improves CMs function when compared with traditional two-dimensional gelatin controls and 3D plain RTG system without CNTs. Therefore, our injectable RTG-CNT system could potentially be used as a minimally invasive tool for cardiac tissue engineering efforts.

Graphical abstract
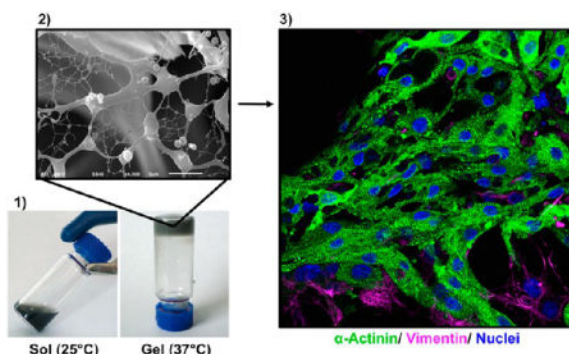
Keywords

cardiac tissue engineering; reverse thermal gel; carbon nanotube; injectable polymer; hybrid-biomimetic hydrogel

INTRODUCTION

Heart failure (HF), a leading cause of death worldwide, is a condition in which the heart is unable to efficiently pump blood to the rest of the body, resulting in progressive cardiomyocyte (CMs) dysfunction and death.[1, 2] Although a number of studies have detected

modest numbers of replicating CMs after cardiac injury, suggesting an attempt at myocardial regeneration,[3] the repair typically occurs through a scarring process leading to tissue fibrosis and loss of function.[4]

Heart transplantation continues to be the gold-standard treatment for end-stage HF.[5, 6] However, complications including the limited availability of donated organs, donor–patient compatibility, immune rejection, and hospitalization costs limit widespread clinical availability.[7, 8]

In light of the limited efficacy of current treatments, direct injection of exogenous cells has been used to repair damaged myocardium. Unfortunately, poor cell survival and retention at the target area limit therapeutic success.[9] In addition, the method of cell delivery and post-transplantation arrhythmias are other major complications for this approach.[10]

As an alternative, various engineered scaffolds have been used to provide a more optimal environment for CMs transplantation. Approaches where CMs are seeded on biomaterial patches have been explored widely,[11–16] although engraftment procedures rely on surgical implantations, and for patients with severe HF, surgical implantation is rarely an option due to various comorbidities.[17–19]

As a minimally invasive alternative, injectable scaffolds have been used to provide a suitable environment for encapsulation of CMs during and after injection into infarcted myocardium.[20–22] In addition, intramyocardial biomaterial injection has the potential to reduce wall stress in the infarct area.[23] Reverse thermal gel (RTG) systems are particularly appealing for cardiac tissue engineering applications, as they undergo reverse phase transition from a hydrophilic solution to a hydrophobic gel solely through temperature stimuli,[24] circumventing the use of ultraviolet radiation or potentially irritating solvents required for other polymeric materials.[20] In addition, gel swelling is not a problem with these systems, since the gelation is driven by hydrophobic interactions.[25] Therefore, RTG systems may provide a minimally invasive, biocompatible, and nontoxic alternative[26] for CMs transplantation strategies.

While polymeric scaffolds may provide essential mechanical support for CMs and the injured myocardium, the majority of the polymeric materials used for tissue engineering are electrically insulated at biologically relevant frequencies[27] and thus do not conduct electrical signals that are critical to cardiac tissue function, such as changes in CMs membrane polarity.[27] To improve the electrical properties of polymeric materials, a number of scaffold systems have incorporated conductive nanoparticles, such as carbon nanotubes (CNTs).[28–31] CNTs have unique electrical, mechanical, and thermal features. Although CNTs present poor solubility and a level of toxicity in the long term, more recent investigations have shown to solve these problems by chemically introducing functional groups.[32] Recently, CMs seeded on rigid substrates demonstrated improvements in viability, proliferation, and maturation compared with traditional CMs culture controls.[11, 33–35]

We previously developed an injectable biomimetic RTG made of poly(serinol hexamethylene urea)-*co*-poly(*N*-isopropylacrylamide) (PSHU–PNIPAAm) functionalized with lysine (RTG-lysine) that was engineered to improve long-term CMs survival. [20] The

RTG-lysine system provides a straightforward delivery vehicle for CMs, as it transitions to a three-dimensional (3D) gel-based matrix seconds after reaching body temperature, enabling 3D CMs growth.[20] In addition, the PSHU backbone of the RTG-lysine contains several free amine groups for further functionalization,[26, 36–39] allowing our system to be amenable for a wide variety of bioconjugations, providing versatility and adaptability for different applications.[20, 26, 36, 40] Moreover, PSHU is also highly biomimetic and biocompatible, since amide ester bonds in the backbone structure provide characteristics similar to those found in natural polymers, such as collagen and gelatin.[20]

In this work, we used the RTG-lysine scaffold as a platform to generate a nanoengineered hybrid RTG-CNT to promote 3D CMs growth, survival, function, and maturation. We found our nanoengineered hybrid 3D RTG-CNT system to be supportive of long-term CMs viability, maturation, and functionality compared with traditional two-dimensional (2D) gelatin-coated dishes and plain 3D RTG-lysine system without CNTs.

MATERIALS AND METHODS

Materials

N-Isopropylacrylamide (NIPAAm), anhydrous N,N-dimethylformamide (DMF), 4,4′-azobis(4-cyanovaleric acid) (CVA), urea, N-BOC-serinol, hexamethylene diisocyanate (HDI), diethyl ether, trifluoroacetic acid (TFA), dichloromethane (DCM), N-(3-(dimethylamino) propyl)-N'-ethylcarbodiimide hydrochloride (EDC-HCl), and L-lysine monohydrochloride were purchased from Sigma-Aldrich, (St. Louis, MO, USA). N-Hydroxysuccinimide (NHS) was purchased from Alfa Aesar (Ward Hill, MA, USA). MWCNTs were purchased from Nanostructured & Amorphous Materials, Inc. (Texas, USA), and all reagents used for the MWCNT functionalization were purchased from Sigma-Aldrich. The filters for MWCNT purification were purchased from Millipore JHWP filters (0.45 μm).

Equipment

Morphological characterization was performed by scanning electron microscopy (SEM) using a JSM-6010LA (JEOL, Tokyo, Japan). Samples were prepared as previously reported.[20, 26, 36, 38, 41] Briefly, the polymers in solution (1% w/w) were allowed to form a gel at 37 °C. Warm water was then put on top, and the samples were frozen immediately by liquid nitrogen immersion. The frozen samples were then lyophilized at –45 °C for 48 h and analyzed by SEM. The storage and loss moduli were measured using an Ares 4400 rheometer (TA Instruments) with an 8 mm parallel plate geometry. A temperature ramp was performed from 25 to 45 °C at a ramp rate of 2 °C at a constant strain rate of 1.0 rad s^{-1} at 0.5% stain (within the viscoelastic regime) to determine gelation as a function of temperature. Experiments were performed in triplicate and averaged. Thermogravimetric analyses (TGA) were performed under a nitrogen flow (60 mL min^{-1}) using a TA Instruments Q500 on sample sizes from 0.7 to 1 mg, and the mass was recorded as a function of temperature. The samples were heated to 100 °C for 20 min and then to 800 °C at 10 °C min^{-1}. Data were interpreted using Thermal Advantage v1.1A software. Transmission electron microscopy (TEM) analyses were performed with a Philips EM 208

microscope with an accelerating voltage of 100 kV (images were acquired using an Olympus Morada CCD camera). CNTs samples were typically suspended in DMF with the help of sonication, and these suspensions were drop-casted on copper or nickel grids (diameter = 3.00 mm, 200 mesh, coated with carbon vacuum overnight, prior to the TEM analysis). Conductivity measurements were performed using a four-probe configuration with a Jandel resistivity meter (RM-3000) linked with a Jandel four-point probe. Resistance measurements were taken with a Protek 6100 multimeter. Briefly, 400 μL of 1.5% (w/w) polymeric solution dissolved in ultrapure water was allowed to gel at 37 °C for 2 min in a 1 × 1 cm mold. Resistance measurements were performed three times for each gel, and measurements were collected in several different areas in the gel. Ultrapure water was used to avoid external ions that may interfere in the material resistance. Resistance measurements were also recorded for CNT-COOH suspended in 400 μL of ultrapure water. Viscosity measurements were performed by using a cone-and-plate digital viscometer (CAP2000+; Brookfield) at 15 °C. Thirty seconds runtime. Dry RTG-lysine or RTG-CNT was dissolved in growth neonatal rat ventricular myocytes (NRVM) media at 1.5% (w/w) and then measured in triplicate at a shear rate of 900 rpm. The viscosity of growth media was also analyzed under the same conditions.

CMs grown on 3D scaffolds for 21 d were characterized for their beating using atomic force microscopy (AFM) JPK NanoWizard 4a, (JPK Instruments USA, Carpenteria, CA) with a Petri dish heater. Briefly, the gel samples were allowed to come back to solution by letting the sample at room temperature for 5 min. The polymer solution was then removed, and the sample was washed with warm media. The cells that migrated to the plate bottom were then analyzed by AFM, by approaching a triangular cantilever with a gold colloidal probe glued at its apex (CP-Au-PNPL-5, NanoandMore), until a force of 0.5 nN was reached. Calibration of the cantilever was made applying the thermal noise method. Beating height was measured for 2.5 s keeping the force exerted by the cantilever as constant.

MWCNT Functionalization

Amino benzyl functionalized carbon nanotubes (200 mg) with a loading of amino groups of 250 μmol g^{-1} were suspended in 200 mL of 1MNaOH (pH 8), and 20 mg of succinic anhydride were added. The suspension was stirred at room temperature for 16 h; it was then filtered on Millipore JHWP filters (0.45 μm) and washed several times with water to neutrality and then with methanol and diethyl ether. The dried powder weighed 205 mg. The powder was characterized by TGA, Kaier test, and TEM.

Polymer Synthesis

RTG-lysine was synthesized as described previously.[20] Briefly, PSHU was synthesized by reacting N-BOC-serinol (1.147 g, 6 mmol), urea (0.36 g, 6 mmol), and HDI (2.018 g, 12 mmol) for 7 d at 90 °C under a nitrogen atmosphere. Anhydrous DMF (6 mL) was used as solvent. The mixture was precipitated into excess anhydrous diethyl ether three times. Unreacted urea was removed by water, and the polymer was lyophilized at −45 °C for 48 h. PSHU was deprotected using 30 mL of TFA/DCM (1:1, v/v) mixture. The deprotection reaction was performed for 45 min at room temperature. The resulting polymer was purified by three precipitations into diethyl ether. PNIPAAm-COOH was synthesized by reacting

NIPAAm (5 g, 800 mmol) and CVA (0.06 g, 4 mmol) for 3 h at 68 °C under nitrogen atmosphere. Anhydrous DMF (10 mL) was used as solvent. The mixture was precipitated into hot water (60 °C). The polymer was then dissolved in ultrapure water and dialyzed (MWCO: 12 000–14 000 Da) for 5 d. The conjugation of PNIPAAm-COOH onto PSHU-NH_2 was performed as follows: PNIPAAm-COOH (0.75 g, 1.21 mmol) was dissolved in 5 mL of anhydrous DMF with five molar excess of EDC-HCl and NHS at room temperature under a nitrogen atmosphere for 24 h. PSHU-NH_2 solution (1 mL, 0.125 gmL^{-1}) prepared in anhydrous DMF was added, and the reaction was performed for 48 h at room temperature under a nitrogen atmosphere. The mixture was precipitated into excess diethyl ether three times. The polymer was then dissolved in ultrapure water and dialyzed (MWCO: 12 000–14 000 Da) for 5 d at room temperature and then filtered through a 2 μm filter. The filtered solution was lyophilized at −45 °C for 48 h. Poly(L-lysine) was synthesized by dissolving L-lysine (0.034 g, 5 mmol) in 5 mL of phosphate-buffered saline (PBS) with five molar excess of EDC-HCl and NHS in a 25 mL round-bottom flask. The mixture was stirred for 15 min at 4 °C. PSHU–PNIPAAm solution (10 mL, 0.1 g mL^{-1}) prepared in PBS was added dropwise, and the reaction was performed for 48 h at room temperature. The polymer was dialyzed (MWCO: 12 000–14 000 Da) for 5 d at room temperature and then filtered through a 2 μm filter. The filtered solution was lyophilized at −45 °C for 48 h. For the CNT conjugation, 300 mg of CNT-COOH was dissolved in 15 mL of anhydrous DMF and sonicated for 30 min. Twenty molar excess of EDC-HCl and NHS was then added, and the mixture was stirred for 15 min at room temperature. RTG-lysine solution (5 mL, 0.1 g mL^{-1}) prepared in anhydrous DMF was added dropwise, and the reaction was performed for 48 h at room temperature. To remove unreacted CNT-COOH, the mixture was centrifuged 5 times at 4000 rpm at 4 °C. Then, the polymer was dialyzed (MWCO: 12 000–14 000 Da) for 5 d at room temperature and lyophilized at −45 °C for 48 h. L-Lysine (0.034 g, 15 mmol) was then added to cover the remaining COOH groups of the CNT. L-Lysine was dissolved in 5 mL of PBS with five molar excess of EDC-HCl and NHS. The mixture was stirred for 15 min at 4 °C. At the same time, the COOH groups of the CNT conjugated to the RTG-lysine were activated with five molar excess of EDC-HCl and NHS. The mixture was stirred for 15 min at 4 °C. The activated L-lysine was then added dropwise to the CNT-RTG, and the reaction was performed for 48 h at room temperature. The polymer was dialyzed (MWCO: 12 000–14 000 Da) for 5 d at room temperature and then lyophilized at −45 °C for 48 h.

Neonatal Rat Ventricular Myocytes Culture

NRVMs were prepared from six, 1–3 d old, pups. All animal studies were performed according to the guidelines of the University of Colorado Denver Animal Care and Use Committee. Briefly, ventricles were separated from the atria using scissors and then dissociated in calcium and bicarbonate-free Hanks with Hepes (CBFHH) buffer containing 500 mg mL^{-1} of collagenase type 2 (Worthington, Biochemical Corporation), and 1 mg/mL of pancreatine. Cardiomyocytes were enriched (>90% purity) over nonmyocytes by two sequential preplating steps on 100 mm dishes in MEM, 4.5 g supplemented with 5% bovine calf serum and 2 mg mL^{-1} vitamin B12 and cultured as previously described.[1] Unattached cells (predominantly myocytes) were collected and cultured in 2D gelatin-coated dishes and into 3D polymeric matrices and then subjected to the different treatments and subsequent

analyses. All experimental conditions were tested in triplicate on at least three independent cell cultures.

3D in Vitro Cell Culture

In vitro 3D culture experiments were performed with the freshly isolated NRVMs by mixing 9×10^4 cells with 150 μL of polymeric solution and allowed to form a gel at 37 °C. Then 100 μL of warm cell culture medium was added on top. Triplicates from at least three independent experiments were analyzed for this study.

Immunocytochemical staining

Immunocytochemistry was performed after 8, 14, and 21 d of culture using the cardiac-specific marker α-sarcomeric actinin 1:100 (Sigma) to assess the contractile apparatus of CMs, vimentin 1:100 (Abcam), a cytoskeleton marker commonly used for fibroblast staining, and CD31 1:100 (Abcam) as marker for endothelial cells. Goat antimouse antibody conjugated to Alexa Fluor 488 (Invitrogen), goat antichicken Cy5 (Abcam), and goat antirabbit antibody conjugated to TRITC (Sigma) were used as secondary antibodies at 1:300. Connexin 43 1:100 (Sigma) was assessed at 21 d to determine the gap junction area between CMs. Goat antirabbit antibody conjugated to Alexa Fluor 594 was used as secondary antibody 1:300 (Invitrogen). 3D and 2D (control) cell cultures were washed twice with warm PBS 1X and then fixed in warm PBS containing 4% PFA for 15 min at 37 °C. Cells were permeabilized with warm 1% Triton X-100 for 1.5 h, blocked in warm 2% BSA in PBS (blocking buffer) for 45 min, and incubated with primary antibodies overnight (all the steps were performed at 37 °C). Secondary antibodies were incubated for 45 min at 37 °C. Cell nuclei were stained with DAPI, and samples were mounted in Vectashield (Vector Laboratories). When indicated and 12 h prior analysis cells were further processed using the Click-IT EdU 555 Imaging kit (Life Technologies) to reveal EdU incorporation, according to the manufacturer's instructions, and stained with DAPI. Fluorescent images were taken from four regions of each sample ($n = 3$) with a Zeiss LSM780 spectral, FLIM, 2P, SHG confocal. Within each experiment, instrument settings were kept constant. To assess the electrical activity of CMs growing in the 3D CNT-RTG and controls, after 21 d of culture, we recorded intracellular calcium signaling of CMs. Cell-permeant fluo 4, AM was added, according to manufacture instructions, to each sample and incubated for 15 min for 2D control groups and 30 min for 3D polymeric groups. Samples were washed three times with warm media before imaging. Calcium transients during spontaneous beating of CMs was recorded using a Zeiss LSM780 confocal and was measured for 20 s. Experiments were performed in triplicate from three independent experiments and averaged. Data were corrected for background epifluorescence.

Statistical Analysis

For all proposed experiments, data were collected in triplicate from at least three independent experiments. ImageJ was used for cell counting in 10 fields per each condition. For calcium transients, signals from myocytes were collected and analyzed from 10 fields per sample and averaged. For the AFM measurements, data were acquired from at least 10 cells per sample and averaged. Statistical significance between experimental groups was

determined using ANOVA. ANOVA Power analysis was completed using GraphPad Prism7software. A *p* value of less than 0.05 was considered statistically significant.

RESULTS AND DISCUSSION

RTG-CNT Synthesis

With the aim of creating a conductive CNT polymer that not only supports CMs survival, maturation, and proliferation but also possesses the advantages of an injectable RTG, we developed a 3D RTG-CNT system using our previously established RTG-lysine as platform.[20]

The reactive groups that can be coupled with amine-containing molecules are by far the most common functional groups present on modification reagents.[42] Carboxylic acid (COOH) groups can be easily conjugated in a high yield to primary amines to form amide linkages by EDC/NHS chemistry.[43] Since the RTG-lysine polymer contains a large number of free primary amine groups,[20] COOH-functionalized CNTs can be chemically conjugated with the polymer (Figure 1A). Therefore, we first began synthetizing CNT with a COOH group by incorporating amino benzyl groups to commercial MWCNT via the diazonium salt arylation reaction route as previously described by Bahr et al.[44] Succinic anhydride was then added to incorporate the COOH groups (Figure 1A). The incorporation of COOH groups in the amino benzyl functionalized CNT was demonstrated by TGA (Figure 1B). The results show a larger weight loss after the reaction with succinic anhydride and the following purification, with a yield of 320 μmol of COOH groups per gram of material. The Kaiser test revealed a residual amount of 25 μmol/g free amino groups, where the initial loading of amino groups was 345 μmol/g, indicating that COOH groups were incorporated into 92.7% of the CNT by mass. This high percentage of COOH in the CNT is ideal to facilitate the chemical conjugation with the RTG-lysine.

CNTs often produce mixtures of solid morphologies that self-associate into aggregates[45, 46] To have an optimal conjugation of CNTs to polymeric materials, it is essential to achieve a uniform dispersion of CNTs in solvents,[45] especially after their functionalization. The dispersion of CNTs-COOH in DMF was analyzed by TEM. Figure 1C shows that the CNTs-COOH were well-dispersed in the solvent, which is ideal for further conjugations. The solubility of our MWCNT-COOH in DMF was then compared with commercial oxidized MWCNT-COOH (Sigma). On the one hand, Supporting Information Figure 1 shows that the commercial oxidized CNTs agglomerate and adsorbed the DMF solvent even after 30 min sonication. On the other hand, our CNTs-COOH were well-dispersed in DMF under the same conditions (30 min of sonication at room temperature).

Our obtained CNTs-COOH were chemically conjugated with the free primary amine group of the RTG-lysine to obtain the RTG-CNT as shown in Scheme 1. Previously optimized concentration of CNTs, as reported by Martinelli et al.,[33–35] were used for the RTG-CNT synthesis.

The 3D morphological characterization of both RTG-lysine and RTG-CNT was performed by SEM. Cross-sectional images of the 3D structure revealed a highly porous configuration

with interconnected porous structures in both RTG systems (Figure 2A). Both appeared to have similar porosity regarding pore size and pore distribution, but the RTG-CNT system presents a fibrous mesh of CNTs among the pores (Figure 2A, bottom right panel). Shin et al. observed a similar fibrous mesh network in GeIMA-CNT hydrogels, which they described to be similar to heart Purkinje fibers.[27] Purkinje fibers are located in the inner heart ventricular walls, where they work as a conductive system, creating synchronized contractions of the right and left ventricles.[47, 48] Similarly, the fibrous CNTs mesh found in our RTG-CNT system may be beneficial for promoting more synchronized CMs contractions and, therefore, may help in the electrophysiological and electromechanical host-cell coupling, which is an area for future investigations.

The sol–gel phase transition and the storage and loss moduli of both RTG-lysine and RTG-CNT were determined using oscillatory shear rheometry (Figure 2B). The sol to gel phase transition was measured using a temperature sweep and determined to be at ~31 °C for gels with and without CNTs, which is near body temperature and ideal for biomedical applications. RTG gels with and without CNTs have viscoelastic properties at 37 °C, where the RTG-CNT presented higher moduli ($G' = 221 \pm 24.6$ Pa, $G'' = 146 \pm 21.6$ Pa) than the RTG-lysine ($G' = 82.0 \pm 4.2$ Pa, $G'' = 48.7 \pm 2.2$ Pa). Therefore, the chemical conjugation of CNT improves the mechanical properties of the RTG system. Although the polymer concentration tested in this investigation makes gels with low stiffness, we previously reported that increasing the polymer concentration in solution increases the mechanical properties of RTG systems,[36] which may be beneficial to provide mechanical support to the wounded heart. Anker et al. reported that alginate hydrogel injected into the left ventricular (LV) heart muscle improved exercise capacity and mitigated symptoms of human subjects with advanced HF.[49] However, the treatment mortality was 8.6%, which indicates that more biocompatible materials are still needed.

Electrical characterization of both the RTG-lysine and RTGCNT systems was performed by conducting resistance measurements (Figure 2C). The RTG-lysine system exhibited a higher resistance at 37 °C than the RTG-CNT and the CNT-COOH in nano pure water (RTG-lysine: 236.8 KΩ ± 3; RTG-CNT 144.3 KΩ ± 4.3; MWCNT-COOH 24.3 KΩ ± 0.64), indicating that the RTG-CNT and CNT-COOH have greater conductance compared to the RTG-lysine. As expected, the CNT-COOH had the lowest resistance, agreeing with previously published studies by Bandaru et al.,[50] while the RTG-CNT had a resistance between the RTG-lysine polymer and the CNT-COOH.

Because of the interest of using the RTG-CNT system for cell delivery, viscosity analysis of both RTG-lysine and RTG-CNT systems were also performed and compared with cell culture media. Figure 2D shows that both RTG-lysine and RTG-CNT solutions at 1.5% present low viscosity, which is beneficial for polymer injection (Supporting Information videos S1 and S2 shows the injection of the polymeric materials through a 31 gauge needle in 37 °C water). (RTG-lysine: 16.78 + 1.2 mPa s; RTG-CNT: 13.4 + 2.5 mPa s; media: 21.9 + 0.8 mPa s).

Therefore, the RTG-CNT, which not only had a higher conductance but also presents better mechanical properties in term of stiffness than the RTG-lysine, and has a low viscosity, holds great promise for use as an injectable material for cardiac tissue engineering.

In Vitro Long-Term NRVMs Survival

We previously reported that NRVMs cultured in 3D using our RTG-lysine system have improved survival, function, and proliferation, all in comparison to traditional 2D gelatin-coated culture-plate and plain RTG.[20] Therefore, we used our RTG-lysine system as a 3D control to assess the biological effects of the RTG-CNT scaffold on NRVMs. Traditional 2D gelatin coating culture dishes, broadly used for NRMV culture and prepared as previously described,[33, 34] were also used as controls.

The organization and phenotype of the NRVMs cultured in 3D using the RTG scaffolds were investigated by immunocytochemistry. Staining for α-sarcomeric actinin, a protein involved in cardiac muscle contraction, was used as cardiac-specific marker. Staining for vimentin, a cytoskeletal fibroblast protein, was used to identify fibroblasts, which typically comprise ~10% of the cell population within our NRVMs isolation protocol.[33, 34] CD31 was used as a marker for endothelial cells, which are not normally present in our current CMs preparation protocol.[20]

On the one hand, as expected, no positive CD31 cells were observed in the cultures. On the other hand, fluorescence microscopy revealed a clear cardiac sarcomere structure represented by cross-striations in NRVMs grown in 3D using both RTG systems (Figure 3A). Even though some fibroblasts were observed in both polymeric scaffolds, most of the cells are CMs as shown by their α-actinin-positive cardiac phenotype during all time points (Figure 3B). In addition, a greater percentage of cells in the RTG systems were α-actinin-positive compared to cells cultured on the 2D gelatin controls. In contrast, the number of fibroblasts significantly increased in the 2D gelatin controls compared with the polymeric systems. Although the original culture percentage of fibroblast increased in the polymeric systems, clearly the polymeric matrix suppressed their long-term proliferation capacity compared with the 2D gelatin controls as has been reported previously.[20] In addition, the microporous architecture of the 3D RTG scaffolds promotes cellular alignment and elongation of both CMs and fibroblasts, which is beneficial for both CMs maturation and improved cell contractility.

However, when comparing the two RTG systems, the percentage of cells that were α-actinin-positive remained nearly constant for all the time points except at day 8, when this value was significantly increased in the RTG-CNT system.

Although most investigations focus on the study of CMs for cardiac tissue remodeling, fibroblasts and endothelial cells are also essential to mimic the native cardiac tissue. Fibroblasts have important functions in the myocardium including electrical coupling with cardiomyocytes and propagation of electrical stimuli. Endothelial cells are required for vascularization.[51] Even though we were not able to find endothelial cells in our cultures, the fact that we can perform a coculture of both CMs and cardiac fibroblast in 3D holds tremendous potential as an emerging artificial cardiac tissue.

We next analyzed the proliferation capacity of NRVMs cultured in the RTG systems and on 2D gelatin controls. Cells were analyzed using a 5-ethynyl-2′-deoxyuridine (EdU) proliferation assay in complete medium at 2, 3, and 4 d postseeding. EdU is an easy and highly sensitive method to label newly synthesized DNA of proliferative cells. In addition, EdU has similar profiles and rates of cell proliferation than other traditional methods such as BrdU[52] and phosphorylated-histone H3 (pHH3),[33, 34] marker of cell division that is only expressed in proliferating cells. We previously analyzed the effect of CNT in the proliferation capacity of CMs using BrdU and pHH3 as markers of cell division.[33, 34] No differences in terms of cell proliferation rates were observed between both markers. Therefore, since EdU has similar rates of cell proliferation than BrdU and PHH3, it was used to label proliferating cells nuclei, while antibodies for α-sarcomeric actinin and vimentin were used to distinguish between cardiac and fibroblast cells, respectively. On the one hand, all culture systems showed EdU incorporation at all time points (Figure 4A, red nuclei). On day 2, there were significantly more proliferating α-sarcomeric actinin-positive cells in the RTG-lysine (39% ± 17.3) than in the RTG-CNT system (15.76% ± 1.27) or on the 2D gelatin controls (8.9% ± 2.1) based on the number of EdU-positive cells (Figure 4B). However, at day 3, the percentage of EdU-positive NRVMs increased to 23.3% ± 7 in the CNT-RTG system. On the other hand, the amount of proliferative NRVMs decreased on the RTG-lysine system to 9.6% ± 4 at day 3. The percentage of proliferative NRVMs growing on gelatin control remained constant at day 3 (6 ± 3). The percentage of EdU- and α-sarcomeric actinin-positive cells progressively decreased over time, reaching the lowest levels for each system at day 4 (2D gelatin controls: 3.8% ± 1; RTG-lysine: 5.0% ± 1.3; RTG-CNT: 15.8% ± 1.6). Since the regenerative capacity of CMs after injury is insufficient for complete heart restoration[3] and because the RTG-CNT system appears to improve the percentage of cardiac cell proliferation in culture over time, this system could be potentially beneficial to promote proliferation of both transplanted CMs and CMs from the native tissue. However, a significant increment of dividing fibroblast was observed at day 2 on the gelatin controls compared with the RTG-CNT and the RTG-lysine systems. No significant differences of dividing fibroblast were observed at days 3 and 4 between the samples.

Since intercellular communication is one of the most important organizational features of the heart,[53–55] we investigated the levels and localizations of the gap-junctions through immunostaining for connexin 43 (Cx43), after cells had been cultured in the RTG-CNT system for 21 d and then compared with 2D gelatin controls and cell cultured in the 3D RTG-lysine. The area of Cx43 in α-actinin-positive cells was quantified by imageJ. Figure 5A shows representative images of NRVMs stained for Cx43 (red) and α-actinin (green) after 21 d of culture in the RTG systems and on 2D gelatin controls. As shown in Figure 5B, we found that NRVMs cultured in the RTG-CNT had the greatest Cx43-positive area (1.87 μm^2 ± 0.36) when compared with 2D gelatin controls (0.25 μm^2 ± 0.1) and the RTG-lysine system (0.88 μm^2 ± 0.13). As expected, NRVMs cultured in the RTG-lysine system also had a significantly greater Cx43-positive area compared with the 2D gelatin controls. On the one hand, several studies have indicated that Cx43 organization is crucial for normal ventricular function and cellular impulse propagation in the healthy human heart.[54, 55] On the other hand, alteration of the Cx43 organization may be one of the main mechanisms leading to arrhythmias.[33] Therefore, the fact that the RTG-CNT systems promote a more organized

area of Cx43 expression may be beneficial in improving the function and integration of transplanted CMs with the host and for the development of functional syncytia.[33]

It has been reported that organized spontaneous intracellular calcium oscillations are correlated with CMs maturation and cell function.[33] To investigate cellular cardiac function, we imaged spontaneous calcium transients to assess NRVMs electrical activity after 21 d of culture (Figure 5C). We found that NRVMs cultured in both 3D RTG-CNT (Supporting Information video s3) and 3D RTG-lysine (Supporting Information video s4) had more frequent calcium oscillations compared to cells cultured on 2D gelatin controls (Supporting Information video s5) and that NRVMs cultured in the 3D RTG-CNT system had more homogeneous calcium oscillations (synchronized beating with similar frequency) compared with the RTG-lysine system. Moreover, 95% of the total cells analyzed (35) in the RTG-CNT system present this synchronized calcium transients profile, where 83% and 94% of the total cells analyzed (35) in the RTG-lysine system and in the gelatin control group, respectively, present a similar calcium transients profile as shown in Figure 5. Therefore, our findings support the idea that the combination of a 3D culture environment and the presence of CNTs may improve CMs intracellular communication and function toward a more mature cardiac phenotype.

Spontaneous beating of NRVMs cultured in the RTG systems and on 2D gelatin controls was also measured by AFM at day 21. Among other applications, AFM can be used to study the biomechanical properties of cells by measuring the deflection of a flexible cantilever while interacting with the cell surface;[56] previous studies have used AFM to successfully measure the altered nuclear mechanical properties of CMs with the cardiomyopathy *LMNA* D192G mutation by AFM.[57] In addition to measuring biomechanical properties of cells, AFM can be used to measure the height of spontaneous beating of CMs (Figure 6A). For our study, we cultured NRVMs in our RTG systems for 21 d and used the reversible property of the gels to retrieve cells for investigation: reducing the temperature to 25 °C, the RTGs became solutions, whereupon CMs migrated to the bottom of the plate, and these were analyzed. The beating activity of NRVMs was registered as peaks in the deflection of the cantilever, giving information about the frequency and height registered during the polarization and depolarization phases. Figure 6B shows the beating activity of CMs cultured in different conditions. Our results obtained with the AFM were similar to those obtained with the calcium transient analysis; therefore, this corroborates the importance of a 3D niche to provide cell support and intracellular communication. However, NRVMs that were growing in the 3D RTG-CNT presented higher contraction while beating (Figure 6B), suggesting that the RTG-CNT niche supports a more efficient CMs contraction.

Our results suggest that the RTG-CNT may be superior to RTG-lysine and the 2D gelatin controls in being supportive of long-term cardiac cell survival (up to 21 d), proliferation, and function, proving that the chemical conjugation of CNT to the RTG-lysine improves the biocompatibility of the system, making the RTG-CNT polymer a promising system for in vivo applications (ongoing study). As previously reported by Martinelli et al., CNTs tightly interact with CMs, penetrating the cell membrane.[34] CNT are cylindrically hollow-shaped nanostructures, made of one or more concentric rolled-up graphene sheets, which possess high surface area.[58, 59] Since CNTs are hollow materials and because we previously

observed a tight CNTs-CMs interaction, it is possible that CNTs may adsorb nutrients from the external media and further act as carriers helping in a more direct cells protein adsorption. In addition, because CNTs are highly electrically conductive materials,[60] several investigations indicate that CNT improve intracellular communication[27, 33] promoting CMs maturation. On the one hand, the precise effects of CNT in CMs are not fully understood and deserve further investigations. On the other hand, the microporous architecture of the 3D RTG scaffolds promotes a more organized cellular alignment mimicking the cardiac tissue as previously reported.[20] Therefore, both 3D RTG niche and CNTs enhance CMs survival, proliferation maturation, and function; however, the use of the RTG-CNT as a cell delivery system in an in vivo model and the understanding of the CNTs effect in CMs maturation, proliferation, and survival needs to be further analyzed.

It is also important to mention that several safety concerns of CNT are often an issue when they are used in biological environments.[61, 32] CNT dispersed in polymeric scaffolds can result in variable toxicity effects, since they can be released from the polymeric matrix.[62] Here, we offer a safer alternative by chemically conjugating CNT into a non-biodegradable material. We previously demonstrated that our RTG systems, with the present chemistry used in this investigation, are non-biodegradable under acidic and enzymatic conditions.[41] This particular characteristic may keep the conjugated CNT in the polymeric matrix. In addition, the MWCNT-COOH synthesis procedure here proposed may avoid further toxic effect caused by metallic impurities and oxidative debris presented in oxidized CNTCOOH.[62] However, as previously mentioned, in vivo studies are required to prove the biocompatibility of the material (ongoing research).

CONCLUSIONS

We have developed an injectable conductive culture system, providing both topographical and electrophysiological cues for native CMs. This system promotes long-term CMs survival with a more aligned cell organization, as observed by immunocytochemistry, and improved cellular function and maturation, as shown by more robust Ca^{2+} transients and stronger contractility by AFM. In addition, the combination of the 3D niche and the CNT favors CMs proliferation and suppresses long-term fibroblast proliferation. Although safety concerns of CNTs are always an issue, here we demonstrated that the chemical conjugation of CNTs to the RTG-lysine system improves CMs survival, proliferation, alignment, and function, proving that the RTG-CNT polymer is non-cytotoxic in vitro. Finally, we believe that this low-viscosity RTG-CNT system that transitions to a 3D matrix by temperature stimuli not only has a tremendous potential for minimally invasive approaches to repair damaged heart tissue but also could be potentially used as 3D scaffold for in vitro investigations.

Supplementary Material

Refer to Web version on PubMed Central for supplementary material.

Acknowledgments

Advanced Microscopy Core for their facilities and support. The authors wish to thank E. P. Wartchow and the Electron Microscopy Lab at Children's Hospital Colorado for facilities and support in the scanning electron microscopy.

ABBREVIATIONS

RTG	reverse thermal gel
CNT	carbon nanotube
3D	three-dimensional
NRVM	neonatal rat ventricular myocytes
TGA	thermogravimetric analysis
SEM	scanning electron microscopy
AFM	atomic force microscopy
CM	cardiomyocytes

References

1. Cahill TJ, Ashrafian H, Watkins H. Genetic Cardiomyopathies Causing Heart Failure. Circ. Res. 2013; 113(6):660–675. [PubMed: 23989711]

2. Mestroni L, Rocco C, Gregori D, Sinagra G, Di Lenarda A, Miocic S, Vatta M, Pinamonti B, Muntoni F, Caforio ALP, McKenna WJ, Falaschi A, Giacca M, et al. Familial Dilated Cardiomyopathy: Evidence for Genetic and Phenotypic Heterogeneity. J. Am. Coll. Cardiol. 1999; 34(1):181–190. [PubMed: 10400009]

3. Eulalio A, Mano M, Dal Ferro M, Zentilin L, Sinagra G, Zacchigna S, Giacca M. Functional Screening Identifies miRNAs Inducing Cardiac Regeneration. Nature. 2012; 492(7429):376–381. [PubMed: 23222520]

4. Van Amerongen MHJ, Engel FB. Features of Cardiomyocyte Proliferation and Its Potential for Cardiac Regeneration: Stem Cells Review Series. J. Cell. Mol. Med. 2008; 12(6A):2233–2244. [PubMed: 18662194]

5. Alraies MC, Eckman P. Adult Heart Transplant: Indications and Outcomes. J. Thorac. Dis. 2014; 6(8):1120–1128. [PubMed: 25132979]

6. Messer S, Large S. Resuscitating Heart Transplantation: The Donation after Circulatory Determined Death Donor. Eur. J. Cardiothoracic Surg. 2016; 49(1):1–4.

7. Garbade J, Barten MJ, Bittner HB, Mohr F-W. Heart Transplantation and Left Ventricular Assist Device Therapy: Two Comparable Options in End-Stage Heart Failure? Clin. Cardiol. 2013; 36(7): 378–382. [PubMed: 23595910]

8. Li S, Loganathan S, Korkmaz S, Radovits T, Hegedus P, Zhou Y, Karck M, Szabó G. Transplantation of Donor Hearts after Circulatory or Brain Death in a Rat Model. J. Surg. Res. 2015; 195(1):315–324. [PubMed: 25592272]

9. Aguado BA, Mulyasasmita W, Su J, Lampe KJ, Heilshorn SC. Improving Viability of Stem Cells During Syringe Needle Flow Through the Design of Hydrogel Cell Carriers. Tissue Eng., Part A. 2012; 18(7–8):806–815. [PubMed: 22011213]

10. Menasché P. Stem Cell Therapy for Heart Failure: Are Arrhythmias a Real Safety Concern? Circulation. 2009; 119(20):2735–2740. [PubMed: 19470902]

11. Kharaziha M, Shin SR, Nikkhah M, Topkaya SN, Annabi N, Dokmeci MR, Khademhosseini A, et al. Biomaterials Tough and Fl Exible CNT E Polymeric Hybrid Scaffolds for Engineering Cardiac Constructs. Biomaterials. 2014; 35(26):7346–7354. [PubMed: 24927679]

12. Herrmann FEM, Lehner A, Hollweck T, Haas U, Fano C, Fehrenbach D, Kozlik-Feldmann R, Wintermantel E, Eissner G, Hagl C, Akra B. In Vitro Biological and Mechanical Evaluation of Various Scaffold Materials for Myocardial Tissue Engineering. J. Biomed. Mater. Res., Part A. 2014; 102(4):958–966.

13. Niu H, Mu J, Zhang J, Hu P, Bo P, Wang Y. Comparative Study of Three Types of Polymer Materials Co-Cultured with Bone Marrow Mesenchymal Stem Cells for Use as a Myocardial Patch in Cardiomyocyte Regeneration. J. Mater. Sci.: Mater. Med. 2013; 24(6):1535–1542. [PubMed: 23620011]

14. Marsano A, Maidhof R, Luo J, Fujikara K, Konofagou EE, Banfi A, Vunjak-Novakovic G. The Effect of Controlled Expression of VEGF by Transduced Myoblasts in a Cardiac Patch on Vascularization in a Mouse Model of Myocardial Infarction. Biomaterials. 2013; 34(2):393–401. [PubMed: 23083931]

15. Fleischer S, Shapira A, Feiner R, Dvir T. Modular Assembly of Thick Multifunctional Cardiac Patches. Proc. Natl. Acad. Sci. U. S. A. 2017; 114:1898. [PubMed: 28167795]

16. Feiner R, Engel L, Fleischer S, Malki M, Gal I, Shapira A, Shacham-Diamand Y, Dvir T. Engineered Hybrid Cardiac Patches with Multifunctional Electronics for Online Monitoring and Regulation of Tissue Function. Nat. Mater. 2016; 15(March):1–8. [PubMed: 26681585]

17. Cheung A, Webb J, Verheye S, Moss R, Boone R, Leipsic J, Ree R, Banai S. Short-Term Results of Transapical Transcatheter Mitral Valve Implantation for Mitral Regurgitation. J. Am. Coll. Cardiol. 2014; 64(17):1814–1819. [PubMed: 25443704]

18. Landes U, Orvin K, Codner P, Assali A, Vaknin-Assa H, Schwartznberg S, Levi A, Shapira Y, Sagie A, Kornowski R. Urgent Transcatheter Aortic Valve Implantation in Patients With Severe Aortic Stenosis and Acute Heart Failure: Procedural and 30-Day Outcomes. Can. J. Cardiol. 2016; 32(6):1–6. [PubMed: 26577892]

19. Schwarz ER, Philip KJ, Simsir SA, Czer L, Trento A, Finder SG, Cleenewerck LA. Maximal Care Considerations When Treating Patients with End-Stage Heart Failure: Ethical and Procedural Quandaries in Management of the Very Sick. J. Relig. Health. 2011; 50(4):872–879. [PubMed: 20191322]

20. Peña B, Martinelli V, Jeong M, Bosi S, Lapasin R, Taylor MRG, Long CS, Shandas R, Park D, Mestroni L. Biomimetic Polymers for Cardiac Tissue Engineering. Biomacromolecules. 2016; 17(5):1593–1601. [PubMed: 27073119]

21. Nelson DM, Ma Z, Fujimoto KL, Hashizume R, Wagner WR. Intra-Myocardial Biomaterial Injection Therapy in the Treatment of Heart Failure: Materials, Outcomes and Challenges. Acta Biomater. 2011; 7(1):1–15. [PubMed: 20619368]

22. Singelyn JM, Christman KL. Injectable Materials for the Treatment of Myocardial Infarction and Heart Failure: The Promise of Decellularized Matrices. J. Cardiovasc. Transl. Res. 2010; 3(5):478–486. [PubMed: 20632221]

23. Singelyn JM, Sundaramurthy P, Johnson TD, Schup-Magoffin PJ, Hu DP, Faulk DM, Wang J, Mayle KM, Bartels K, Salvatore M, Kinsey AM, Demaria AN, Dib N, Christman KL. Catheter-Deliverable Hydrogel Derived from Decellularized Ventricular Extracellular Matrix Increases Endogenous Cardiomyocytes and Preserves Cardiac Function Post-Myocardial Infarction. J. Am. Coll. Cardiol. 2012; 59(8):751–763. [PubMed: 22340268]

24. Park MH, Joo MK, Choi BG, Jeong B. Biodegradable Thermogels. Acc. Chem. Res. 2012; 45(3): 424–433. [PubMed: 21992012]

25. Park D, Weinman CJ, Finlay JA, Fletcher BR, Paik MY, Sundaram HS, Dimitriou MD, Sohn KE, Callow ME, Callow JA, Handlin DL, Willis CL, Fischer DA, Kramer EJ, Ober CK. Amphiphilic Surface Active Triblock Copolymers with Mixed Hydrophobic and Hydrophilic Side Chains for Tuned Marine Fouling-Release Properties. Langmuir. 2010; 26(12):9772–9781. [PubMed: 20359178]

26. Peña B, Shandas R, Park D. A Heparin-Mimicking Reverse Thermal Gel for Controlled Delivery of Positively Charged Proteins. J. Biomed. Mater. Res., Part A. 2015; 103(6):2102–2108.

27. Shin SR, Jung SM, Zalabany M, Kim K, Zorlutuna P, Kim SB, Nikkhah M, Khabiry M, Azize M, Kong J, Wan KT, Palacios T, Dokmeci MR, Bae H, Tang X, Khademhosseini A. Carbon-Nanotube-Embedded Hydrogel Sheets for Engineering Cardiac Constructs and Bioactuators. ACS Nano. 2013; 7(3):2369–2380. [PubMed: 23363247]

28. Pok S, Vitale F, Eichmann SL, Benavides OM, Pasquali M, Jacot JG. Biocompatible Carbon Nanotube-Chitosan Scaffold Matching the Electrical Conductivity of the Heart. ACS Nano. 2014; 8(10):9822–9832. [PubMed: 25233037]

29. Hopley EL, Salmasi S, Kalaskar DM, Seifalian AM. Carbon Nanotubes Leading the Way Forward in New Generation 3D Tissue Engineering. Biotechnol. Adv. 2014; 32(5):1000–1014. [PubMed: 24858314]

30. Mooney E, Mackle JN, Blond DJP, O'Cearbhaill E, Shaw G, Blau WJ, Barry FP, Barron V, Murphy JM. The Electrical Stimulation of Carbon Nanotubes to Provide a Cardiomimetic Cue to MSCs. Biomaterials. 2012; 33(26):6132–6139. [PubMed: 22681974]

31. Bhatia SK. Tissue Engineering for Clinical Applications. Biotechnol. J. 2010; 5(12):1309–1323. [PubMed: 21154670]

32. Fabbro A, Bosi S, Ballerini L, Prato M. Carbon Nanotubes: Artificial Nanomaterials to Engineer Single Neurons and Neuronal Networks. ACS Chem. Neurosci. 2012; 3(8):611–618. [PubMed: 22896805]

33. Martinelli V, Cellot G, Fabbro A, Bosi S, Mestroni L, Ballerini L. Improving Cardiac Myocytes Performance by Carbon Nanotubes Platforms. Front. Physiol. 2013; 4:1–6. [PubMed: 23372552]

34. Martinelli V, Cellot G, Toma FM, Long CS, Caldwell JH, Zentilin L, Giacca M, Turco A, Prato M, Ballerini L, Mestroni L. Carbon Nanotubes Instruct Physiological Growth and Functionally Mature Syncytia: Nongenetic Engineering of Cardiac Myocytes. ACS Nano. 2013; 7(7):5746–5756. [PubMed: 23734857]

35. Martinelli V, Cellot G, Toma FM, Long CS, Caldwell JH, Zentilin L, Giacca M, Turco A, Prato M, Ballerini L, Mestroni L. Carbon Nanotubes Promote Growth and Spontaneous Electrical Activity in Cultured Cardiac Myocytes. Nano Lett. 2012; 12(4):1831–1838. [PubMed: 22432413]

36. Laughter MR, Ammar DA, Bardill JR, Pena B, Kahook MY, Lee DJ, Park D. A Self-Assembling Injectable Biomimetic Microenvironment Encourages Retinal Ganglion Cell Axon Extension in Vitro. ACS Appl. Mater. Interfaces. 2016; 8(32):20540–20548. [PubMed: 27434231]

37. Yun D, Famili A, Lee YM, Jenkins PM, Freed CR, Park D. Biomimetic Poly(serinol Hexamethylene Urea) for Promotion of Neurite Outgrowth and Guidance. J. Biomater. Sci., Polym. Ed. 2014; 25(March):354–369. [PubMed: 24279744]

38. Yun D, Laughter MR, Park D. A Biomimetic Reverse Thermal Gel for 3-Dimensional Neural Tissue Engineering. Austin J. Biomed. Eng. 2014; 1(4):1–5.

39. Jenkins PM, Laughter MR, Lee DJ, Lee YM, Freed CR, Park D. A Nerve Guidance Conduit with Topographical and Biochemical Cues: Potential Application Using Human Neural Stem Cells. Nanoscale Res. Lett. 2015; 10(1):972. [PubMed: 26071111]

40. Yun D, Lee YM, Laughter MR, Freed CR, Park D. Substantial Differentiation of Human Neural Stem Cells into Motor Neurons on a Biomimetic Polyurea. Macromol. Biosci. 2015; 15(9):1206–1211. [PubMed: 26033933]

41. Famili A, Kahook MY, Park D. A Combined Micelle and Poly(serinol Hexamethylene Urea)-Co-Poly(N-Isopropylacrylamide) Reverse Thermal Gel as an Injectable Ocular Drug Delivery System. Macromol. Biosci. 2014; 14(12):1719–1729. [PubMed: 25187427]

42. Alexander, GN. Bioconjugate Techniques. Hermanson; 1996.

43. Wang C, Yan Q, Liu HB, Zhou XH, Xiao SJ. Different EDC/NHS Activation Mechanisms between PAA and PMAA Brushes and the Following Amidation Reactions. Langmuir. 2011; 27(19): 12058–12068. [PubMed: 21853994]

44. Bahr JL, Tour JM. Covalent Chemistry of Single-Wall Carbon Nanotubes. J. Mater. Chem. 2002; 12(7):1952–1958.

45. Porrelli D, Cok M, Abrami M, Bosi S, Prato M, Grassi M, Paoletti S, Donati I. Evaluation of Concentration and Dispersion of Functionalized Carbon Nanotubes in Aqueous Media by Means of Low Field Nuclear Magnetic Resonance. Carbon. 2017; 113:387–394.

46. Zhou J, Chen J, Sun H, Qiu X, Mou Y, Liu Z, Zhao Y, Li X, Han Y, Duan C, Tang R, Wang C, Zhong W, Liu J, Luo Y, Mengqiu Xing M, Wang C. Engineering the Heart: Evaluation of Conductive Nanomaterials for Improving Implant Integration and Cardiac Function. Sci. Rep. 2015; 4(1):1–11.

47. Boyden PA, Dun W, Robinson RB. Cardiac Purkinje Fibers and Arrhythmias; The GK Moe Award Lecture 2015. Hear. Rhythm. 2016; 13(5):1172–1181.

48. Brunello L, Knollmann BC, Janssen PML, Gyorke S. Relative Contribution of Purkinje Fibers to CA(2+) - Dependent Arrhythmias in a Murine Model of CPVT. Biophys. J. 2014; 106(2):112A–112A.

49. Anker SD, Coats AJS, Cristian G, Dragomir D, Pusineri E, Piredda M, Bettari L, Dowling R, Volterrani M, Kirwan BA, Filippatos G, Mas JL, Danchin N, Solomon SD, Lee RJ, Ahmann F, Hinson A, Sabbah HN, Mann DL. A Prospective Comparison of Alginate-Hydrogel with Standard Medical Therapy to Determine Impact on Functional Capacity and Clinical Outcomes in Patients with Advanced Heart Failure (AUGMENT-HF Trial). Eur. Heart J. 2015; 36(34):2297–2309. [PubMed: 26082085]

50. Bandaru PR. Electrical Properties and Applications of Carbon Nanotube Structures. J. Nanosci. Nanotechnol. 2007; 7(4):1239–1267. [PubMed: 17450889]

51. Vunjak-Novakovic G, Tandon N, Godier A, Maidhof R, Marsano A, Martens TP, Radisic M. Challenges in Cardiac Tissue Engineering. Tissue Eng., Part B. 2010; 16(2):169–187.

52. Sun X, Zhang C, Jin H, Sun G, Tian Y, Shi W, Zhang D. Flow Cytometric Analysis of T Lymphocyte Proliferation in Vivo by EdU Incorporation. Int. Immunopharmacol. 2016; 41:56–65. [PubMed: 27816727]

53. Severs NJ, Bruce AF, Dupont E, Rothery S. Remodelling of Gap Junctions and Connexin Expression in Diseased Myocardium. Cardiovasc. Res. 2008; 80(1):9–19. [PubMed: 18519446]

54. Severs NJ, Coppen SR, Dupont E, Yeh HI, Ko YS, Matsushita T. Gap Junction Alterations in Human Cardiac Disease. Cardiovasc. Res. 2004; 62(2):368–377. [PubMed: 15094356]

55. Kostin S, Dammer S, Hein S, Klovekorn WP, Bauer EP, Schaper J. Connexin 43 Expression and Distribution in Compensated and Decompensated Cardiac Hypertrophy in Patients with Aortic Stenosis. Cardiovasc. Res. 2004; 62(2):426–436. [PubMed: 15094362]

56. Lanzicher T, Martinelli V, Long CS, Del Favero G, Puzzi L, Borelli M, Mestroni L, Taylor MRG, Sbaizero O. AFM Single-Cell Force Spectroscopy Links Altered Nuclear and Cytoskeletal Mechanics to Defective Cell Adhesion in Cardiac Myocytes with a Nuclear Lamin Mutation. Nucleus. 2015; 6(5):394–407. [PubMed: 26309016]

57. Lanzicher T, Martinelli V, Puzzi L, Del Favero G, Long CS, Mestroni L, Taylor MRG, Sbaizero O, et al. The Cardiomyopathy Lamin A/C D192G Mutation Disrupts Whole-Cell Biomechanics in Cardiomyocytes as Measured by Atomic Force Microscopy Loading-Unloading Curve Analysis. Sci. Rep. 2015; 5(1):1–14.

58. Fabbro A, Sucapane A, Toma FM, Calura E, Rizzetto L, Carrieri C, Roncaglia P, Martinelli V, Scaini D, Masten L, Turco A, Gustincich S, Prato M, Ballerini L. Adhesion to Carbon Nanotube Conductive Scaffolds Forces Action-Potential Appearance in Immature Rat Spinal Neurons. PLoS One. 2013; 8(8):1–14.

59. Aqel A, El-Nour KMMA, Ammar Raa, Al-Warthan A. Carbon Nanotubes, Science and Technology Part (I) Structure, Synthesis and Characterisation. Arabian J. Chem. 2012; 5(1):1–23.

60. Bosi S, Fabbro A, Ballerini L, Prato M. Carbon Nanotubes: A Promise for Nerve Tissue Engineering? Nanotechnol. Rev. 2013; 2(1):47–57.

61. Bianco A, Kostarelos K, Prato M. Making Carbon Nanotubes Biocompatible and Biodegradable. Chem. Commun. 2011; 47(37):10182–10188.

62. Lalwani G, D'Agati M, Khan AM, Sitharaman B. Toxicology of Graphene-Based Nanomaterials. Adv. Drug Delivery Rev. 2016; 105:109–144.
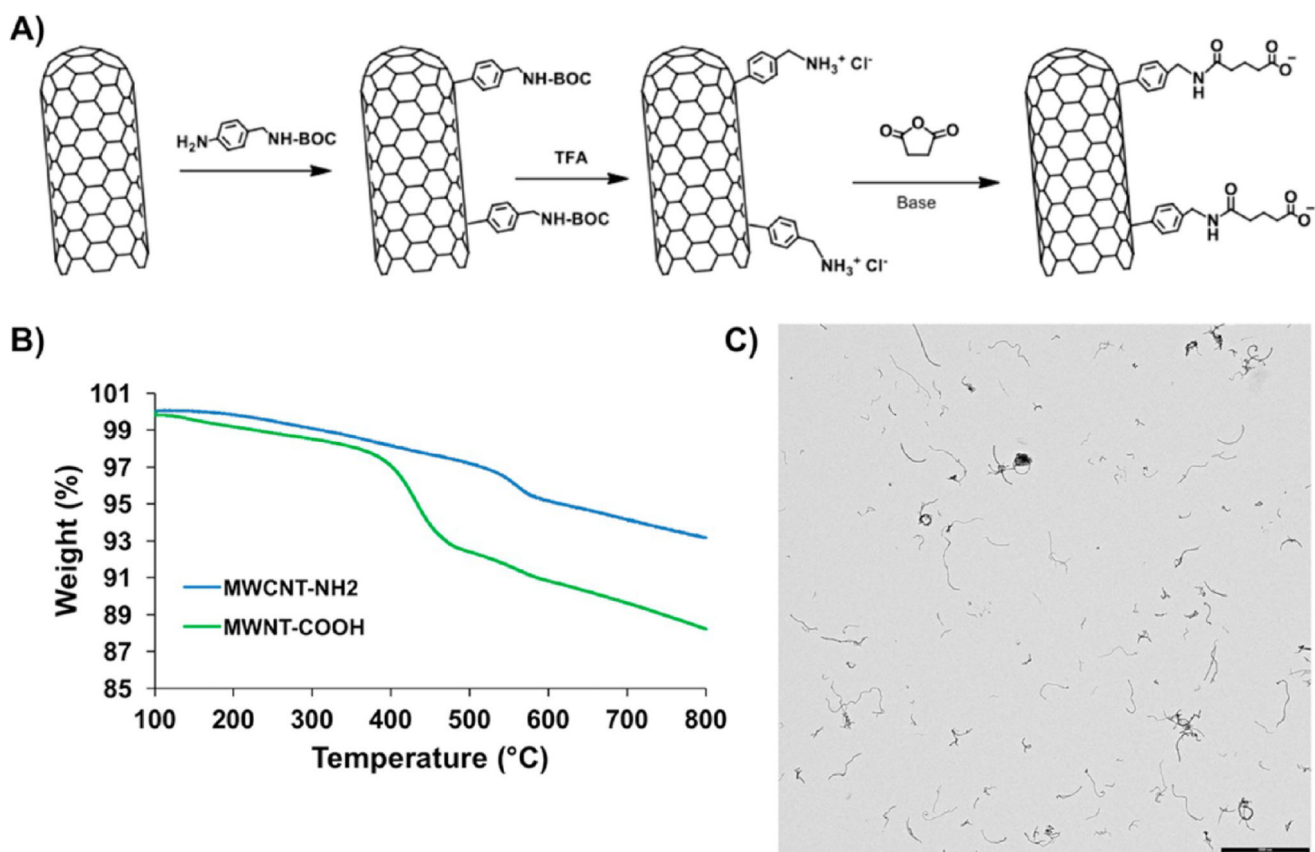
Figure 1.
MWCNT-COOH. (A) Schematic representation of MWCNT-COOH synthesis. (B) TGA of MWCNT-NH2 (blue) and MWCNT-COOH (green). (C) TEM shows MWCNT-COOH dispersion in DMF. Scale bar 2000 nm.
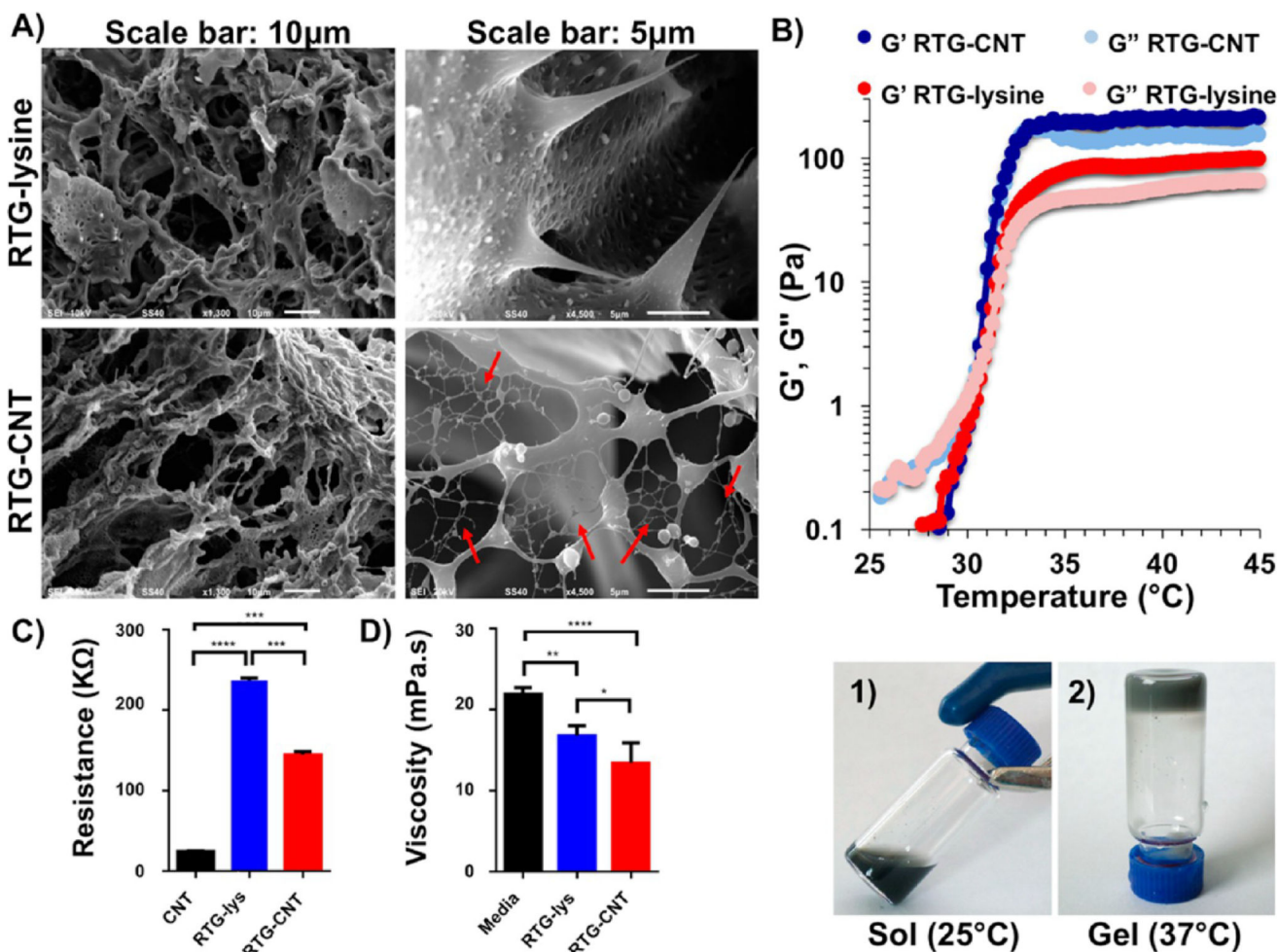
Figure 2.

(A) Cross-section micrographs of the RTG systems at different magnifications. (top) RTG-lysine and (bottom) RTG-CNT. A fibrous CNT mesh network can be observed in the RTG-CNT system (red arrows). (B) Storage and loss moduli of both RTG-lysine (red) and RTG-CNT (blue) and temperature-dependent phase transition: the chemical conjugation of CNT improves the mechanical properties of the RTG-lysine system. (bottom, 1) An aqueous solution of RTG-CNT at room temperature turns to (bottom, 2) physical gel at 37 °C. (C) Resistance measurements: the hybrid CNT-RTG presented a resistance between both the RTG polymer and the CNT-COOH. (ANOVA-Dunn's test) (CNT-COOH "vs" RTG-lysine ****p value: <0.0001; $n = 20$; RTG-lysine "vs" RTG-CNT ***p value: 0.0002; $n = 20$; RTG-CNT "vs" CNT-COOH ***p value: 0.0002, $n = 20$). (D) Both RTG systems present lower viscosity than media. (ANOVA-Bonferroni's test) (media "vs" RTG-lysine **p value: 0.0013; $n = 5$; RTG-lysine "vs" RTG-CNT *p value: 0.0238; $n = 5$; RTG-CNT "vs" media ****p value: <0.0001, $n = 5$).
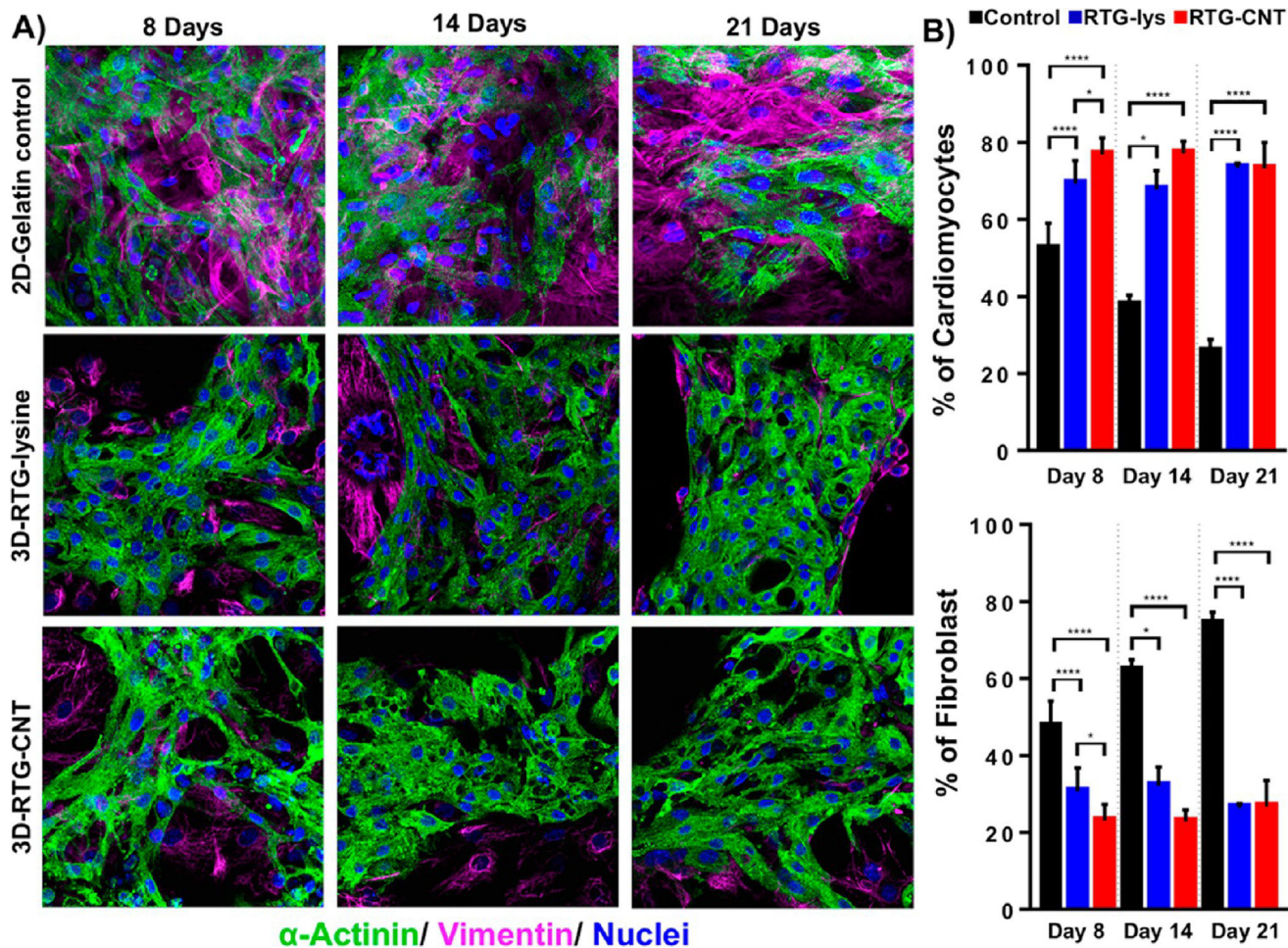
Figure 3.

Fluorescence staining of NRVMs and fibroblasts cultured in different substrates. Sarcomeric α-actinin (green), vimentin (pink), and DAPI (blue). (A, top) NRVMs cultured on 2D gelatin control. (A, middle) NRVMs cultured in 3D RTG-lysine. (A, bottom) NRVMs cultured in 3D RTG-CNT. (B) Quantification of the percentage of NRVMs and fibroblast growing in gelatin-control and the RTG systems. Significant differences on the % of NRVMs can be observed at all the time points between the gelatin control group and RTG systems. (ANOVA-Bonferroni's test). Day 8: RTG-lysine "vs" gelatin control ****p value: <0.0001; $n = 8$; RTG-CNT "vs" gelatin control ****p value: <0.0001; $n = 8$; RTG-CNT "vs" RTG-lysine *p value: <0.018; $n = 8$. (ANOVA-Dunn's test) Day 14: RTG-lysine "vs" gelatin control *p value: 0.0487, $n = 8$; RTG-CNT "vs" gelatin control ****p value: <0.0001, $n = 8$. (ANOVA-Bonferroni's) Day 21: RTG-lysine "vs" gelatin control ****p value: <0.0001, $n = 8$; RTG-CNT "vs" gelatin control ****p value: <0.0001, $n = 8$. Significant differences on the % of fibroblast were also observed at all time points between the gelatin control group and RTG systems. (ANOVA-Bonferroni's test) Day 8: RTG-lysine "vs" gelatin control ****p value: <0.0001, $n = 8$; RTG-CNT "vs" gelatin control ****p value: <0.0001 $n = 8$. RTG-CNT "vs" RTG-lysine *p value: 0.018 $n = 8$. (ANOVA-Dunn's test) Day 14: RTG-lysine "vs" gelatin control *p value: 0.0487, $n = 8$; RTG-CNT "vs" gelatin control ****p value: <0.0001 $n = 8$. (ANOVA-Bonferroni's test) Day 21: RTG-lysine "vs" gelatin control ****p

value: <0.0001; n = 8; RTG-CNT "vs" gelatin control ****p value: <0.0001; n = 8. Data are presented as mean ± standard deviation (SD).
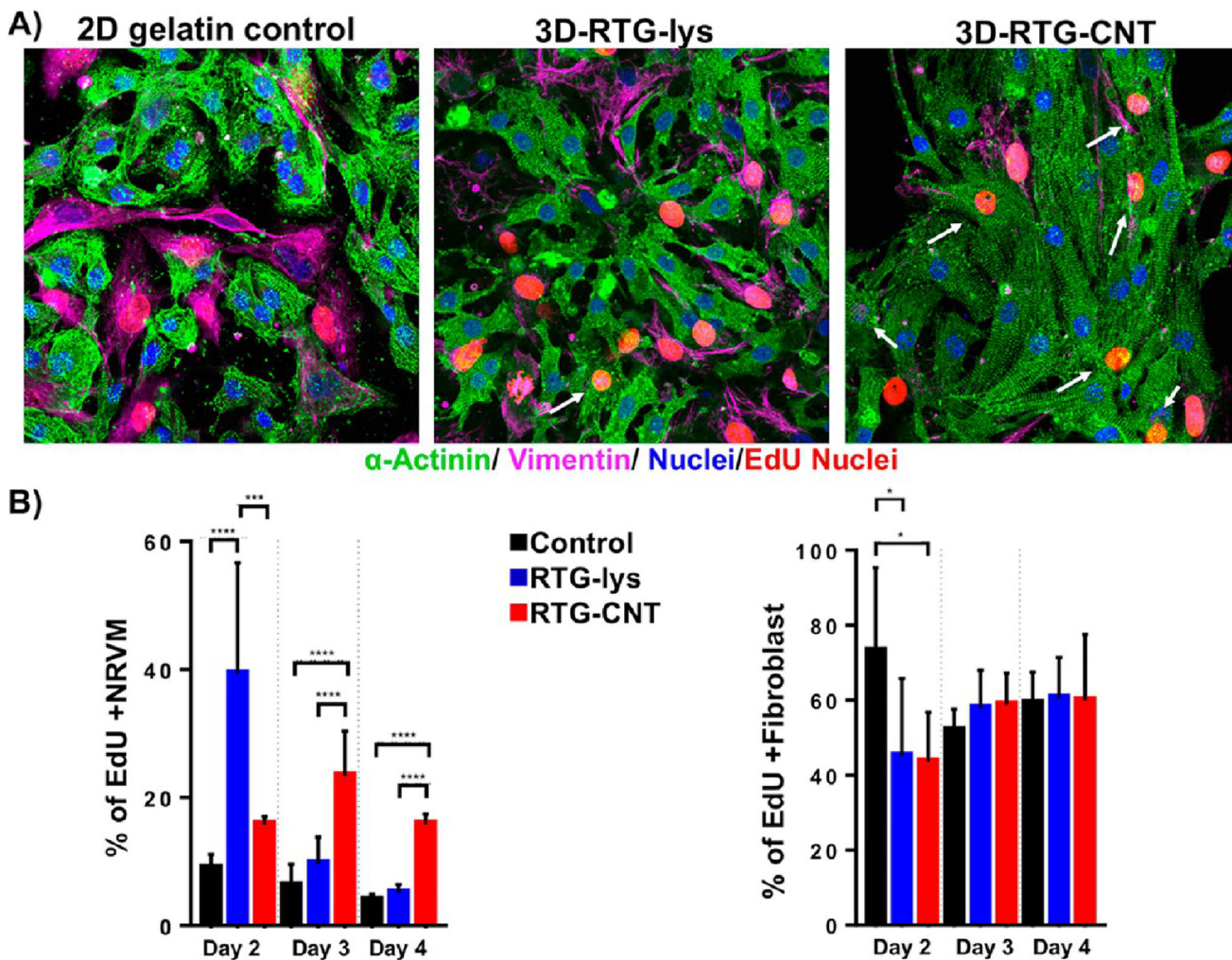
Figure 4.
Proliferation assay of NRVMs and fibroblasts. (A, left to right) NRVMs and fibroblast cultured on 2D gelatin control, 3D RTG-lysine and 3D RTG-CNT at day 4. (B) Significant differences of dividing NRVMs on the RTGlysine system were observed at day 2 when compared with the gelatin controls (****p value: <0.0001, $n = 8$) and with the RTG-CNT scaffold (***p value: 0.0004, $n = 8$). Significant differences of dividing NRVMs on the RTG-CNT system were observed at days 3 and 4 when compared with the gelatin control and the RTG-lysine system. Day 3: RTG-CNT "vs" gelatin control ****p value: <0.0001, $n = 8$; RTG-CNT "vs" RTG-lysine ****p value: <0.0001, $n = 8$. Day 4: RTG-CNT "vs" gelatin control ****p value: <0.0001, $n = 8$; RTG-CNT "vs" RTG-lysine ****p value: <0.0001, $n = 8$; significant differences of dividing fibroblast were observed at day 2 between the gelatin controls and the RTG polymers. Day 2: gelatin control "vs" RTG-lysine *p value: 0.0241, $n = 8$; gelatin control "vs" RTG-CNT *p value: 0.0166, $n = 8$. Data are presented as mean ± SD.
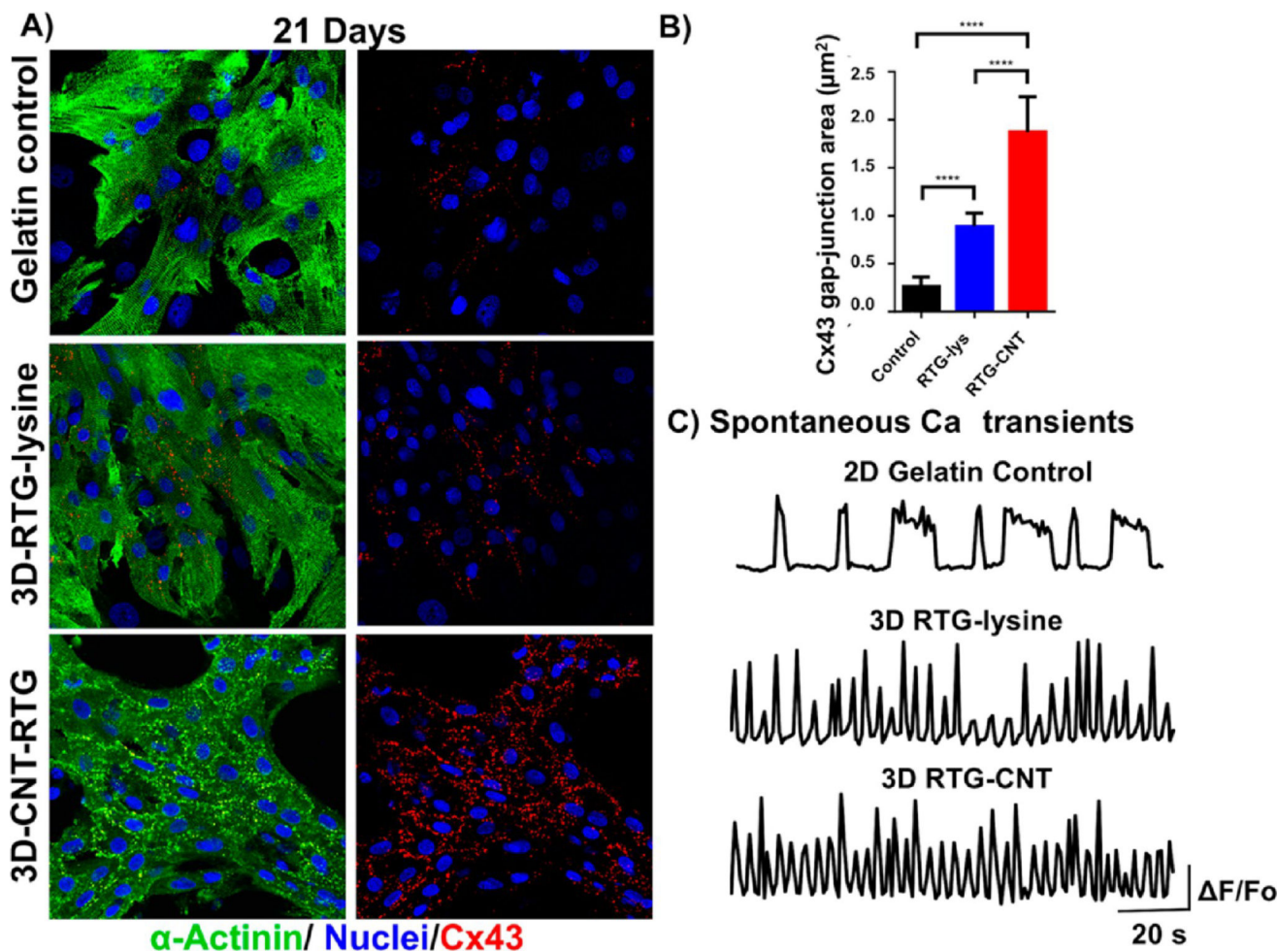
Figure 5.
Intercellular communication of NRVMs growing in different substrates after 21 d of culture.
(A) Fluorescence images of connexin 43 (red dots), sarcomeric α-actinin (green), and DAPI
(blue) staining of NRVMs (top) NRVMs cultured on 2D gelatin control; (middle) NRVMs
cultured in 3D RTG-lysine; (bottom) NRVMs cultured in 3D RTG-CNT. (B) Quantification
of Cx43 gap junction area: Significant differences on Cx43 gap-junction were observed
between the gelatin control groups and the RTG systems. RTG-lysine "vs" gelatin control
****p value: <0.0001, $n = 8$; RTG-CNT "vs" gelatin control ****p value: <0.0001, $n = 8$;
RTG-CNT "vs" RTG-lysine ****p value: <0.0001, $n = 5$. Data are presented as mean ± SD
($n = 5$). (ANOVA-Bonferroni's test). Data are presented as mean ± SD ($n = 5$). (C)
Spontaneous calcium transients of NRVMs growing on 2D gelatin control and in 3D RTG
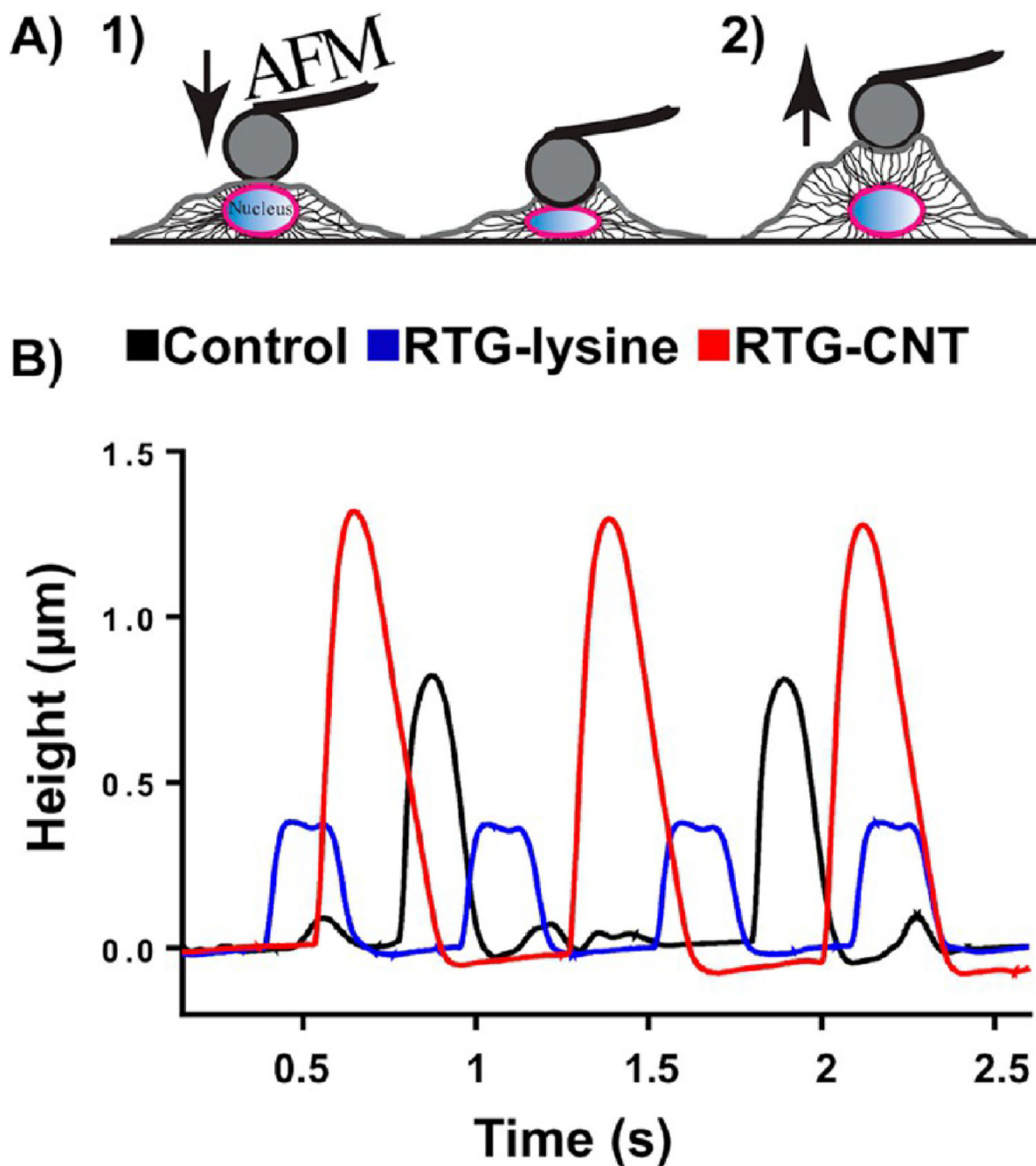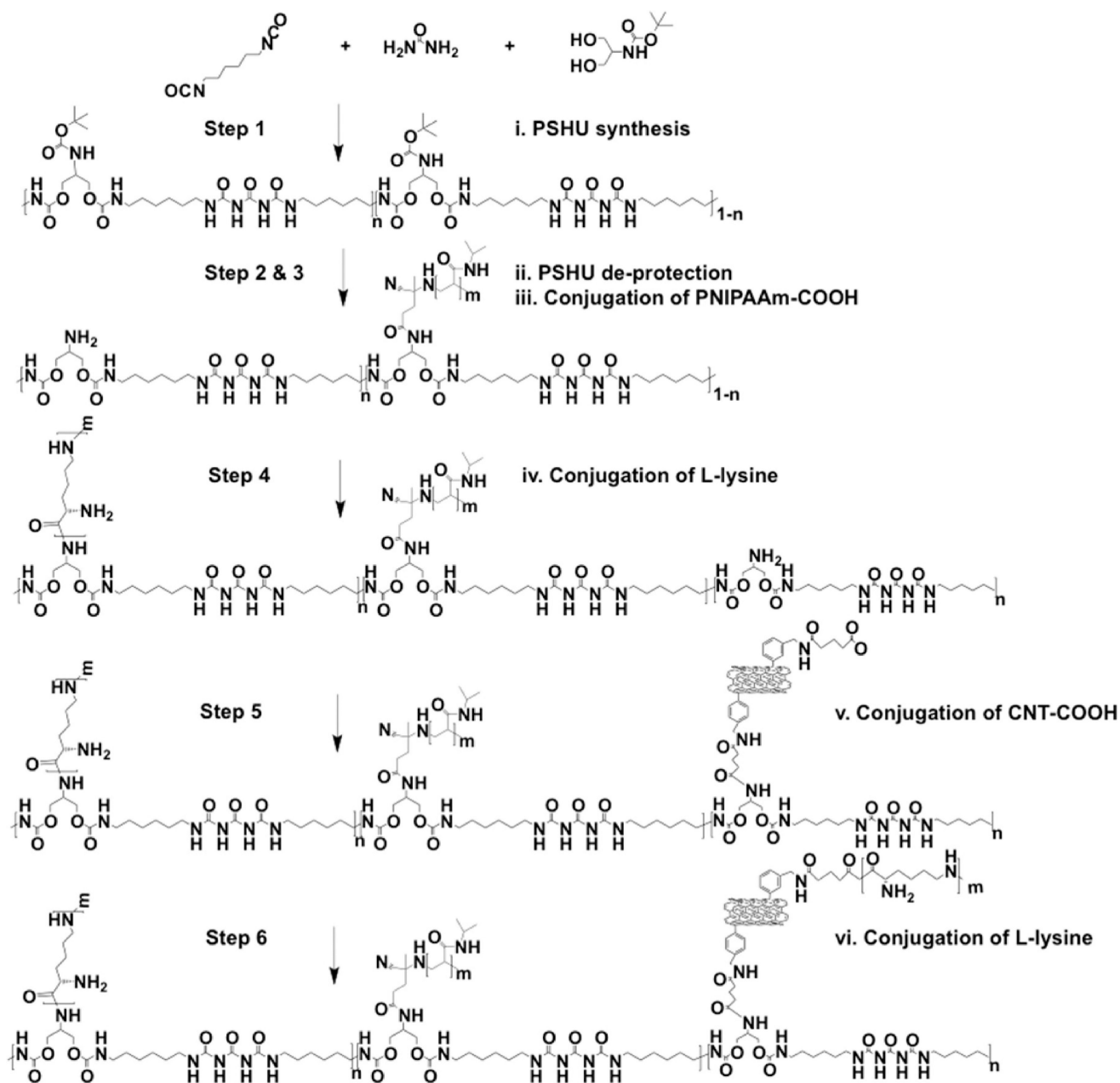systems ($n = 5$).

Figure 6.
Spontaneous beating of NRVMs cultured for 21 d in different substrates by AFM. (A) Schematic representation of the beating activity of NRVMs measurements by the deflection of the AFM cantilever. (left to right) AFM cantilever gently pushing the nuclear region the CM, the beating activity of CM pushed away the AFM cantilever, providing information about beating height and frequency. (B) NRVMs cultured in the 3D RTG-CNT presented higher contraction, while beating suggesting that the CNT-RTG niche supports a stronger cardiomyocyte contraction.

Scheme 1.
RTG-CNT Synthesis